Effects of the Nature of the Starting Population on the Properties of Rugate Filters Designed with the Genetic Algorithm

Pieter L. Swart, Abraham P. Kotzé, and Beatrys M. Lacquet

***Abstract*—The genetic algorithm optimization technique for optical filter design is applied to two starting populations, an inverse Fourier transform population and a random population. The refractive index profiles after convergence, and the transmittance of the filter outside the region of support, are markedly different in the two cases. The Fourier filter has lower sidelobes and fails gracefully outside the region of support whereas the random filter fails catastrophically in this wavelength region. The ripple in the passband is higher for the random filter. Furthermore, the average value of refractive index profile and the excursion in refractive index are much larger for the filter generated with the random starting population. However, most of the drawbacks of the random starting population are eliminated by chromosome manipulation in the spatial frequency domain. The filter properties after this intervention approximate those of the Fourier filter.**

***Index Terms*—Chromosome manipulation, genetic algorithm, optical filter, refractive index profile.**

I. Introduction

The advent of wavelength-division multiplexing (WDM) in fiber-optic communication systems has led to a requirement for various wavelength selective devices such as narrow-band filters [1], [2]. The wavelength selectivity can be obtained by dielectric filters, coupled wave devices or diffractive elements such as Bragg gratings [3]. Dielectric filters may be of the high–low stack variety or of quasicontinuous inhomogeneous layers such as rugate filters. We have a research program in the design and manufacture of rugate filters for optical fiber applications. The design of rugate filters is somewhat more complex than the discrete high–low index type filters [4]. Several design techniques have evolved such as classical rugate design [5], inverse Fourier transform [6], [7], wavelet based design [8], and the genetic algorithm [9]. This paper reports on the effect of the nature of the starting population on the properties of rugate filters designed with the genetic algorithm. The genetic algorithm or GA is not strictly a design algorithm but rather a refinement technique [9]. Therefore, it needs a set of initial designs (the starting population) that are subsequently refined. These starting populations have a definite influence on the convergence rate of the algorithm and the quality of the final design. We present data on the design of a 100-nm wide 50% beamsplitter centered at 980 nm, which employs two families of starting populations. We are also introducing a novel procedure to enhance the performance of the GA with random starting population.

Manuscript received July 2, 1999; revised February 24, 2000. This work was supported by TELKOM SA, ATC (Pty) Ltd. and the Department of Trade and Industry through their THRIP program.

The authors are with the Centre for Optical Communications, Faculty of Engineering, Rand Afrikaans University, Auckland Park 2006, South Africa (e-mail: PLS@ing1.rau.ac.za).

Publisher Item Identifier S 0733-8724(00)05074-X.

II. The Genetic Algorithm

The GA optimization technique is modeled on the evolution of living organizms [10]. The GA presumes that the solution to an optimization problem is an individual that can be defined by a set of parameters [10]. Its basic building block is an alphabet letter or nucleotide. For a thin-film filter this represents any physical property such as the refractive index, extinction coefficient, positional index and thickness of a sublayer. The combination of two or more alphabet letters forms a codon. A codon can be, for example, the set containing the refractive index value, the physical thickness, and the absorption coefficient of a sublayer in a filter. A set of N codons forms a chromosome, with N being the number of sublayers in the filter. Lastly, a set of chromosomes forms the starting population that the genetic algorithm uses to generate new generations either by mutating a single chromosome or by combining two or more chromosomes. This population is allowed to compete in an environment in which the strongest or best individuals in the population have a better chance of survival into the next generation. The GA evaluates the fitness of a chromosome by using an evaluation or merit function [10]. A suitable merit function used to return a single number reflecting the total fitness of a specific chromosome is given by [11]

$$F = \sqrt{\frac{1}{M}\sum_{j=1}^{M}\left(\frac{T_T(\lambda_j) - T_A(\lambda_j)}{dT_j}\right)^2} \tag{1}$$

with F the figure of merit, $T_T(\lambda_j)$ the desired target transmittance of the filter at wavelength λ_j, $T_A(\lambda_j)$ the actual transmittance of the filter, and dT_j the tolerance.

III. Starting Populations

A starting population may be compiled by a number of methods ranging from analytical methods such as the inverse Fourier transform and the classical rugate design, to knowledge-based systems [4], and to randomly created filters [10]. For the purposes of this paper we examined two of these populations. The first population was compiled by using the inverse Fourier transform synthesis technique given by [6], [7]

$$\int_{-\infty}^{\infty} \frac{dn}{dx}\,\frac{1}{2n}\,e^{ikx}\,dx = Q(k)e^{i\phi(k)} \tag{2}$$

with $Q(k)$ an even function of the desired transmittance, $\phi(k)$ a phase function, $n(x)$ the refractive index profile, $k = 2\pi/\lambda$ the free-space wave number, and x twice the optical distance from the geometrical centre of the inhomogeneous layer

$$x = 2\int_0^z n(u)\,du \tag{3}$$

with z the depth variable. Population diversity was obtained by using several phase and Q functions [6], [7]. The parameters in the phase functions were selected in a random fashion. The second starting population was created by random selection of the refractive index alphabet letter in each gene for fixed values of the corresponding thickness of the sublayer. We used a uniform probability distribution with mean value $n_a = 2.35$, standard deviation $\sigma = 0.5$, but limited to the refractive index range from 1.5 to 3.2. The optical thickness alphabet letter in each codon was set at the same fixed value for both the inverse Fourier transform and the random starting populations. We applied quintic matching layers [12], each with an optical thickness of 2 μm, between the filter and the incident and exit media.

IV. The Design Process

The design process was implemented as follows: The desired transmittance spectrum was generated over the 0.7–1.3 μm wavelength range [7], called the region of support, and saved for later reference. The following constraints were placed on the starting populations: Each chromosome comprised 300 codons with a total optical thickness of 22 μm. This translates into a physical thickness alphabet letter of approximately 30 nm for each sublayer. The refractive index alphabet letter was restricted to any value of refractive index within the range of $1.5 \leq n \leq 3.2$. This corresponds to the values of refractive index obtainable with SiN_xO_y grown in our electron cyclotron resonance plasma enhanced chemical vapor deposition system (ECR-PECVD) [13], [14]. For each of the starting populations 150 chromosomes were generated, and the tolerance dT_j was set equal to 1%. For the implementation of the GA, the crossover and mutation probabilities were set at 0.6 and 0.05 respectively. The matrix method was used to calculate the corresponding reflectance and transmittance of each filter chromosome [15]. The design process was implemented in MATLAB.[1]

V. Results and Discussion

The filter obtained by initiating the GA with the inverse Fourier transform starting population refractive index profile (Fourier filter) after 10 000 generations is shown in Fig. 1(a), and its corresponding transmittance and reflectance in Fig. 1(b) and (c) respectively. Fig. 2(a)–(c) depicts the refractive index profile, the corresponding transmittance and the reflectance of the filter obtained from the GA started with the random starting

[1]MATLAB is a registered trademark of MathWorks, Inc., Natick, MA USA.

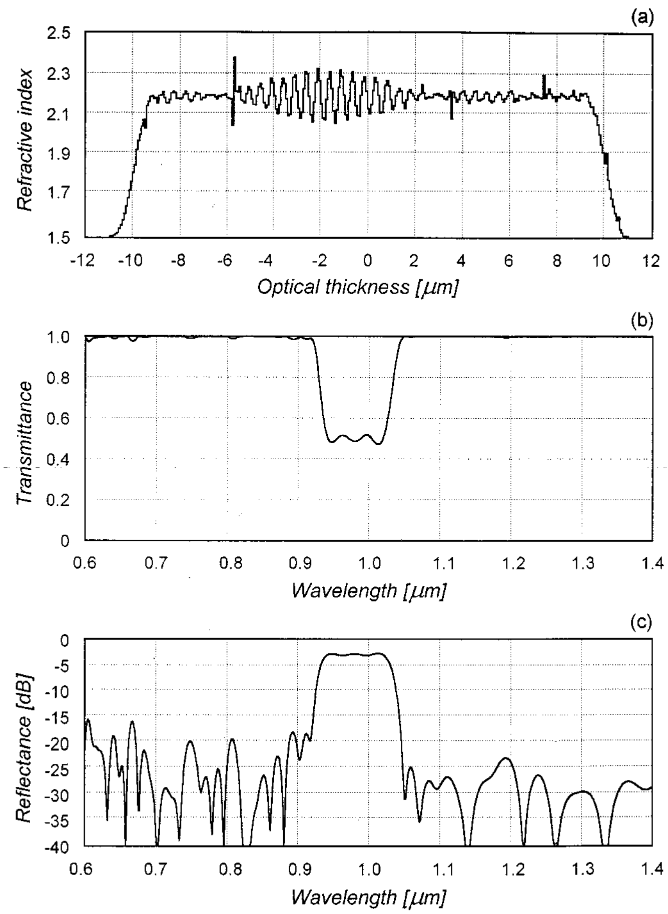

Fig. 1. (a) Refractive index profile generated by initiating the GA with an inverse Fourier transform starting population after 10 000 new generations. (b) Corresponding transmittance spectrum of the filter. (c) Corresponding reflectance spectrum of the filter.

population (stochastic filter), respectively. These results also pertain to 10 000 generations. Fig. 3 shows the convergence rates of the figure of merit for both filters.

We make the following observations from Figs. 1–3: The average value of the refractive index of the Fourier filter is 2.19 in comparison with the 2.33 of the stochastic filter. Also, the refractive index variation in the Fourier filter is between 2.05–2.39, whereas it varies from 1.60 to 3.20 for the stochastic filter. The Fourier filter has a smaller ripple in the beamsplit band ($\pm 2.3\%$ compared with $\pm 2.7\%$) and a lower reflectance outside the beamsplit band (less than -18.5 dB, compared with -15.9 dB for the stochastic filter). The filter obtained by starting the GA with the inverse Fourier transform population (Fourier filter) fails gracefully outside the region of support (design region) from 0.7 to 1.3 μm. This is in sharp contrast to the filter obtained with the random population (stochastic filter). It has high reflectance bands between 0.6–0.7 μm, and between 1.3–1.4 μm.

The Fourier filter has a much faster convergence rate (dashed line) for the figure of merit than that of the stochastic filter (solid line). After fewer than 20 new generations of the Fourier filter, its figure of merit is already smaller than the stochastic filters figure of merit after 10 000 new generations. The overall fitness

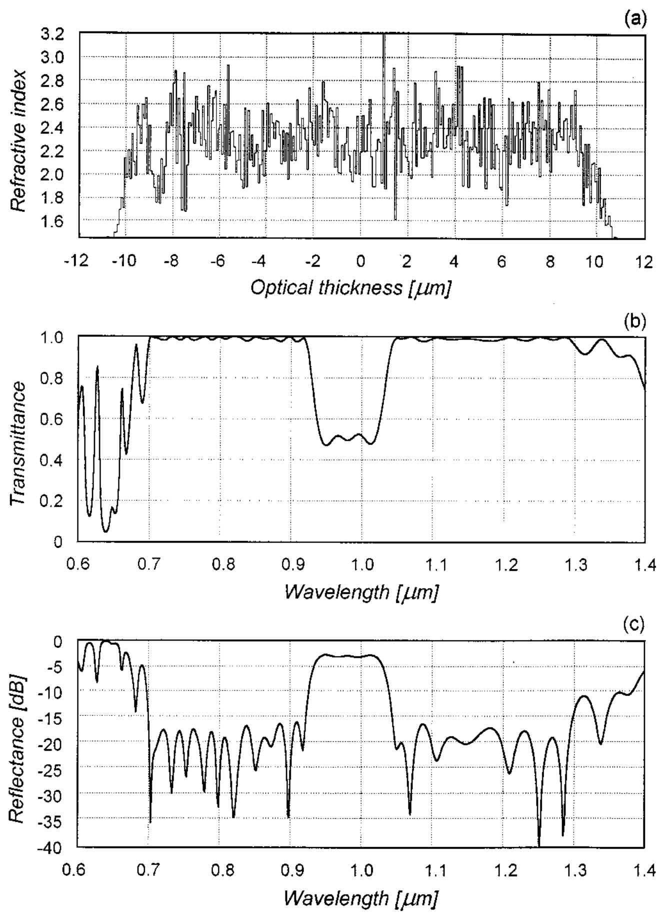

Fig. 2. (a) Refractive index profile generated by initiating the GA with a random starting population after 10 000 new generations. (b) Corresponding transmittance spectrum of the filter. (c) Corresponding reflectance spectrum of the filter.

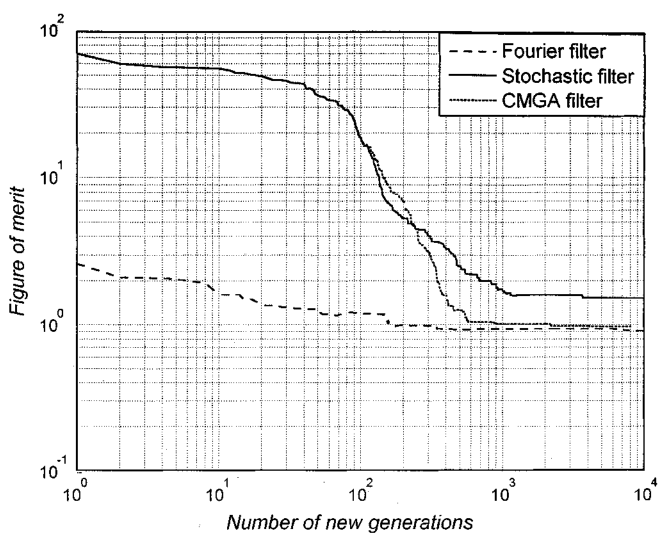

Fig. 3. Convergence rates of the figure of merit for the filters with an inverse Fourier transform starting population (dashed line), a random starting population (solid line), and a chromosome-modified filter with random starting population (dotted line).

of the Fourier filter $(F = 0.91)$, as represented by the figure of merit after 10 000 generations, is significantly better than the corresponding value for the stochastic filter $(F = 1.52)$.

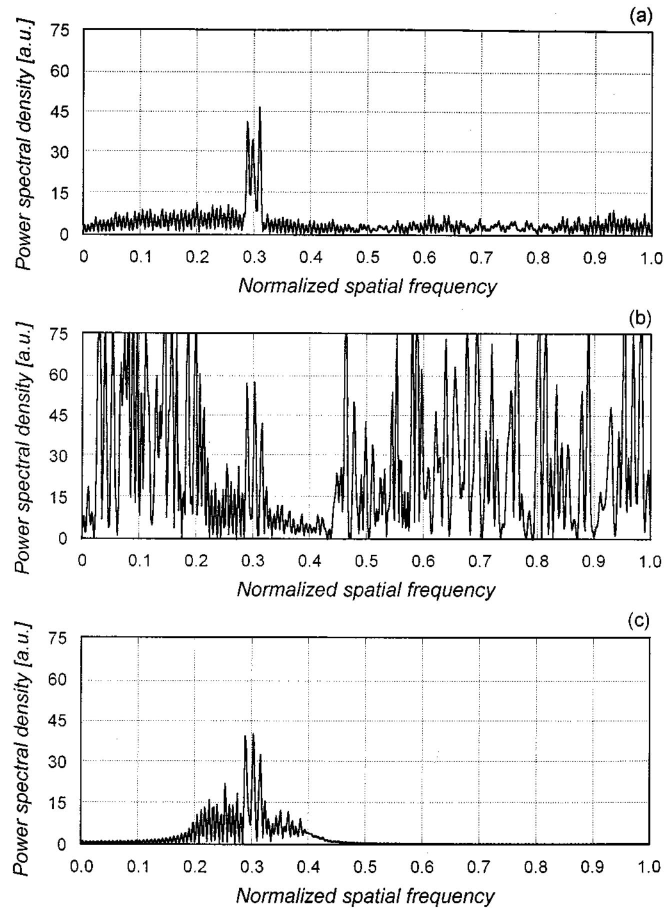

Fig. 4. Power spectral density of the refractive index profiles after10 000 new generations of (a) the Fourier filter, (b) the stochastic filter, and (c) the stochastic filter after bandpass filtering.

The question of whether the two filters generated from the two different starting populations approach the same global solution still remains to be answered. Although the transfer functions look very similar in the region of support, it is difficult to compare the refractive index profiles. The stochastic filter has a large random component that masks the filter chromosome. The underlying structure of the chromosome is conveyed much better in the spatial frequency domain. Fig. 4(a) and (b) shows the power spectral density of the refractive index profiles of the Fourier and stochastic filter respectively. It is clear from these spectra that the key spatial frequency information lies in the spatial frequency range of approximately 0.2–0.42 (normalized with respect to the Nyquist frequency). This point is illustrated well by filtering the refractive index profile of the stochastic filter. Fig. 4(c) shows the power spectral density obtained by processing the data with a 20th-order Butterworth bandpass filter with a passband of 0.2–0.42. Similar to the Fourier filter, this spectrum also contains three prominent peaks around the normalized frequency of 0.3. The filtered refractive index profile and its transmittance and reflectance are displayed in Fig. 5(a)–(c) respectively. Although it is clearly not the same refractive index profile, there are similarities in the envelopes. The stochastic filter seems to be an approximate transpose of the Fourier filter. We think this similarity is fortuitous. It is

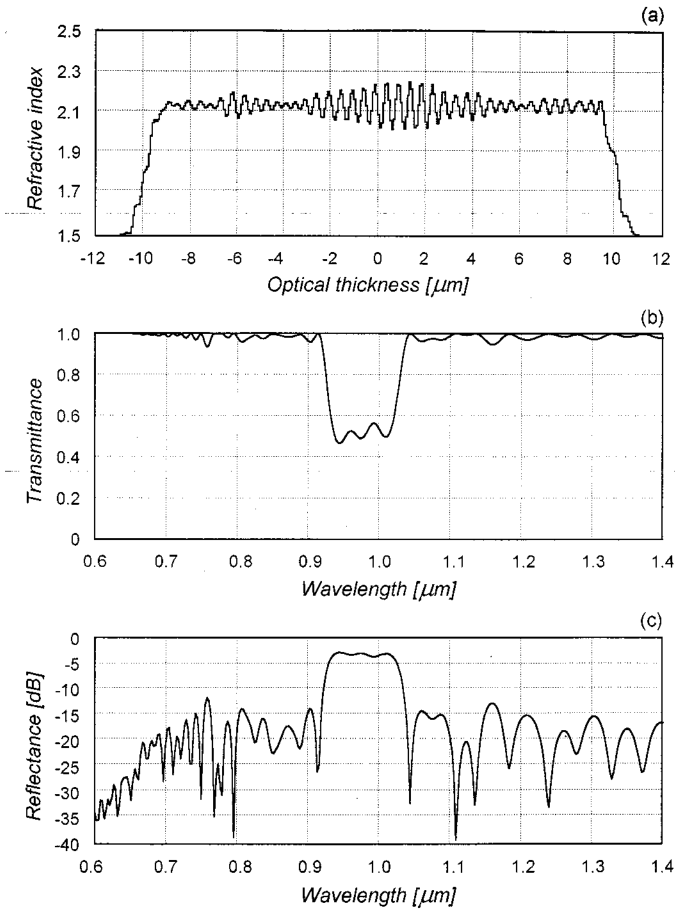

Fig. 5. (a) Refractive index profile generated by initiating the GA with a random starting population. The profile generated after 10 000 generations was bandpass filtered with a 20th-order Butterworth filter with a passband from 0.2 to 0.42. (b) Corresponding transmittance spectrum of the filter. (c) Corresponding reflectance spectrum of the filter.

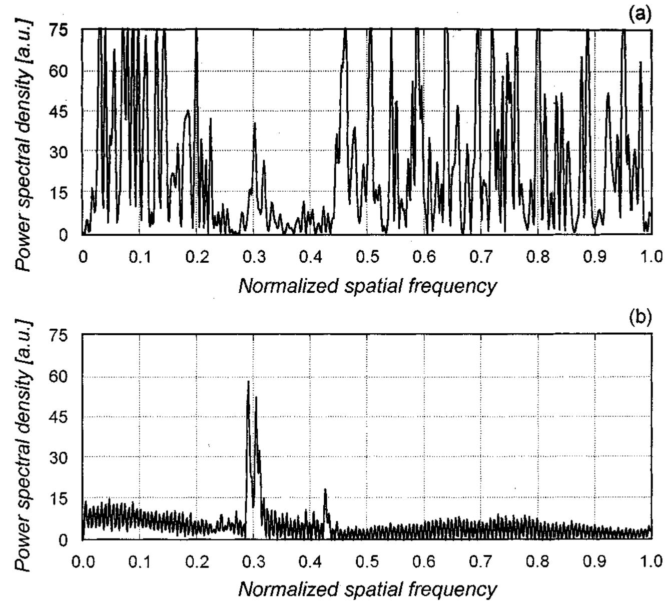

Fig. 6. Power spectral density of the refractive index profile of (a) the stochastic filter after 100 generations, and (b) the chromosome-manipulated filter after 8000 new generations. The chromosome manipulation was performed after 100, 200, and 400 generations.

well known [16] that the inverse problem (i.e., synthesis of the refractive index profile from a given reflectance function) is unique only if a minimum phase function (zeros restricted to one half of the complex frequency plane) is assumed. As we do not have control over the phase function in the genetic algorithm, the solution space consists of numerous minima corresponding to arbitrary phase functions.

We tested the robustness of the GA by initializing the algorithm with 46 different random populations and by running each population for 2000 generations. All of the filters have figures of merit that cluster around a mean value of 1.56. The standard deviation is 0.15. These results confirm that the GA is very robust as it apparently reached one of the global minima for each of the 46 random starting populations used.

VI. Chromosome Manipulation

The process of bandpass filtering of the refractive index profile as discussed in the previous paragraphs suggests a novel procedure to enhance the performance of the GA with random starting populations. If the chromosomes can be modified by bandpass filtering early in the evolutionary cycle, the stochastic

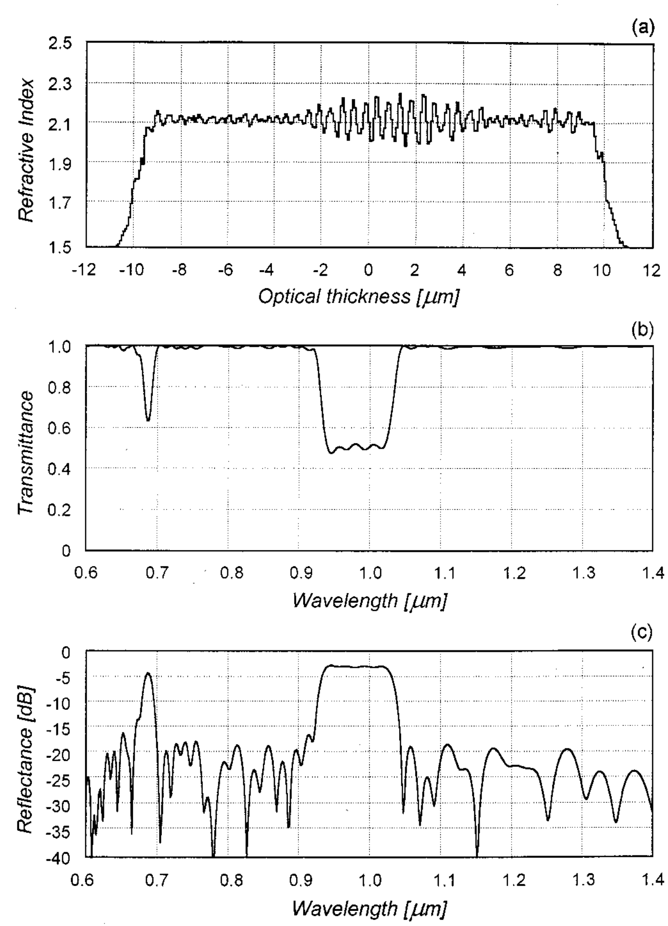

Fig. 7. (a) Refractive index profile of the CGMA after 8000 new generations. (b) Corresponding transmittance spectrum of the filter. (c) Corresponding reflectance spectrum of the filter.

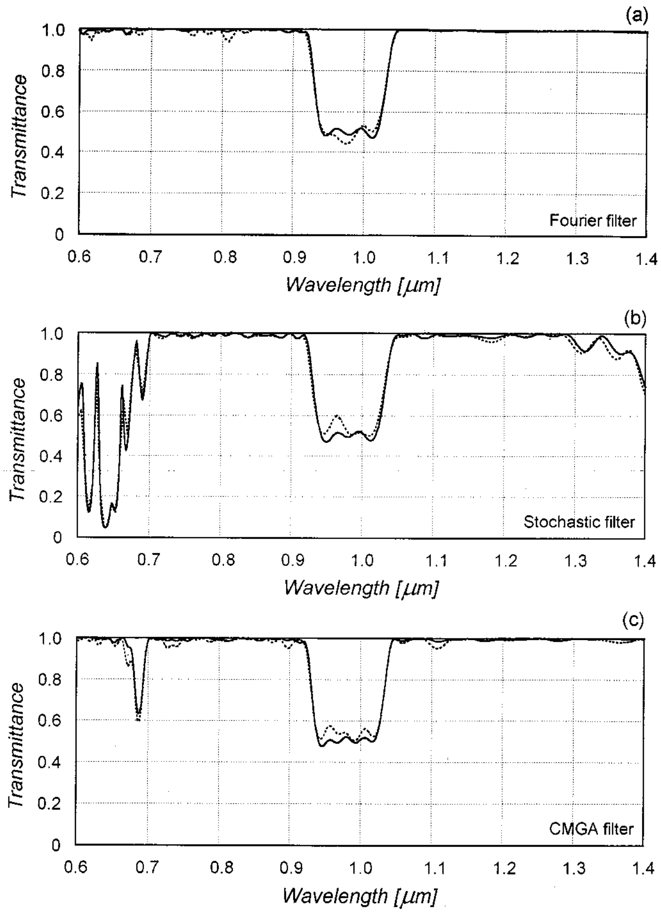

Fig. 8. Effect of normally distributed random perturbations in the refractive index profile on the transmittance of the filter generated by initiating the GA with (a) and inverse Fourier transform starting population, (b) a random starting population, and (c) a random starting population with chromosome manipulation after 100, 200, and 400 generations. The dashed curves depict transmittance for the perturbed filters.

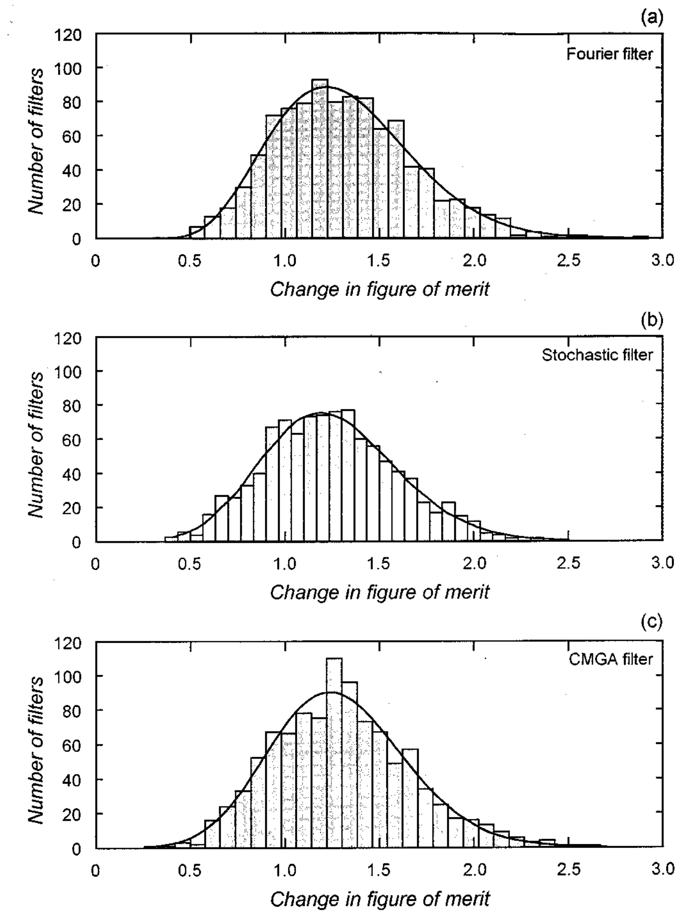

Fig. 9. Distribution of the changes in the figure of merity for normally distributed perturbations in the refractive index profile of filters generated by initiating the GA with (a) an inverse Fourier transform starting population, (b) a random starting population, and (c) a random starting population with chromosome manipulation after 100, 200, and 400 generations.

or noise components of the population can be reduced. This should improve the convergence, the final figure of merit and the performance outside the region of support. It is clear from Fig. 6(a) that the signal component and the noise component of the refractive index power spectral density can be clearly distinguished after as few as 100 generations. Based on this observation we implemented the stochastic GA with chromosome manipulation (CMGA) as follows: the entire population was filtered after 100 generations with the bandpass filter as described in Section V. This procedure was repeated after 200 and again after 400 generations, and then the GA was allowed to evolve for a total of 8000 generations.

The rate of convergence is significantly improved as can be seen from the dotted curve in Fig. 3. The figure of merit reached a value of 0.96 after 8000 generations. This compares favorably with the figure of merit of 0.91 of the Fourier filter after the same number of generations, and it is significantly better than the stochastic filter after 10 000 generations. $(F = 1.52.)$ Fig. 6(b) depicts the power spectral density of the chromosome manipulated stochastic filter after 8000 generations. Its refractive index profile and transmittance and reflectance are shown in Fig. 7.

We make the following observations from Fig. 7. The average value of the refractive index of the CMGA filter is 2.13 in comparison to the 2.33 of the stochastic filter. The refractive index variation of the CMGA filter is between 2.00–2.25, whereas it varies from 1.60 to 3.20 for the stochastic filter. The CMGA filter has a somewhat smaller ripple in the beamsplit band ($\pm 2.2\%$ compared with $\pm 2.7\%$) and lower reflectance outside the beamsplit band (less than -16.5 dB compared with -15.9 dB for the stochastic filter). Similar to the Fourier filter, the CMGA also fails gracefully outside the region of support (design region) from 0.7 to 1.3 μm, except for a single peak at 0.69 μm.

VII. Sensitivity

One can expect random variations in the refractive index profile of ECR-PECVD grown films of up to 1%. We have studied the effect of process variations on the three filters numerically by using a normal distribution of refractive index variations with a standard deviation equal to 1% of the mean value of the refractive index profile. This implies in practice that refractive index variations of up to 4% will occur. This is larger than can be reasonably expected, but it was chosen to make the effects more visible. Each of the filter profiles were perturbed with these random variations, and the reflectance, transmittance and figure of merit were computed. This procedure was repeated a thousand times. The effect of such perturbations on the Fourier transform, stochastic and chromosome-manipulated filters is shown for a typical filter in Fig. 8(a)–(c), respectively. Fig. 9(a)–(c) shows the distributions of the changes in the figure of merit for each of these filters. These distributions are skew and cannot be well represented by Gaussian functions. We obtained the best fits in the least squares sense by beta functions of the form [17]

$$y = cx^{a-1}(1-x)^{b-1} \tag{4}$$

where a, b and c are adjustable constants. The average figure of merit for the Fourier transform starting population is degraded by $\Delta F = 1.32$, for the stochastic filter by $\Delta F = 1.24$, and for the chromosome-manipulated stochastic filter by $\Delta F = 1.30$. The corresponding standard deviations were 0.37, 0.35, and 0.36. These deleterious effects are mostly manifested by an increase in the passband ripple to ± 0.22 dB for the Fourier filter, to ± 0.45 dB for the stochastic filter, and to ± 0.35 dB for the chromosome-manipulated filter. The mean values of the reflectance changed from -3.0 dB to -3.1 dB, -3.2 dB, and -3.4 dB, respectively. We do not as yet have an explanation for the detailed behavior of the three filter types with random perturbations applied to their refractive index profiles.

VIII. Conclusion

The starting population used in the GA optimization technique has a marked influence on the final refractive index profile as well as the transmittance of the filter outside the region of support, and the ripple in the passband. This was demonstrated by a 3-dB beamsplitter designed for 980 nm. Furthermore, the filter realized by application of the GA to the stochastic starting population has large refractive index excursions in consecutive layers. This can be detrimental to the filter performance as it may lead to increased film stress which may lead to delamination at high power densities. In addition, it will complicate the manufacturing process as the film composition will have to change drastically from sublayer to sublayer. The sensitivity of the filters to random changes in the refractive index of the sublayers is not overly influenced by the nature of the starting population.

We introduced a new technique of chromosome manipulation where a random starting population was used and the chromosomes were subjected to a bandpass filter early in the evolutionary cycle. This intervention improved the rate of convergence of the merit function, the final figure of merit and the ripple in the passband. The variation in the refractive index profile became much smaller, and the filter failed gracefully outside the region of support. For instances where the inverse Fourier transform synthesis technique is not appropriate to generate a starting population, the CMGA technique could be used as an alternative.

References

[1] M. S. Borella, J. P. Jue, D. Banerjee, B. Ramamurthy, and B. Mukherjee, "Optical components for WDM lightwave networks," *Proc. IEEE*, vol. 85, pp. 1274–1307, Aug. 1997.

[2] B. E. Lemoff, L. B. Aronson, and L. A. Buckman, "SpectraLan: A low-cost multiwavelength local area network," *Hewlett-Packard J.*, vol. 48, no. 5, pp. 42–52, 1997.

[3] J. J. Pzn and Y. Shi, "Dense WDM multiplexer and demultiplexer with 0.4 nm channel spacing," *Electron. Lett.*, vol. 34, no. 1, pp. 74–74, 1998.

[4] P. Baumeister, "Design of optical multilayer coatings," in *Proc. SPIE Optical Interference Coatings*, F. Abeles, Ed. Grenoble, France, 1994, vol. 2253, pp. 2–9.

[5] W. E. Johnson and R. L. Crane, "Introduction to rugate filter technology," in *Proc. SPIE Inhomogeneous and Quasi-Inhomogeneous Optical Coatings*, J. A. Dobrowolski and P. G. Verly, Eds. Bellingham, WA, 1993, vol. 2046, pp. 88–108.

[6] P. V. Bulkin, P. L. Swart, and B. M. Lacquet, "Fourier transform design and ECR-PECVD manufacturing of lossy optical coatings with inhomogeneous refractive index," *Appl. Opt.*, vol. 35, no. 22, pp. 4413–4419, 1996.

[7] H. Fabricius, "Gradient-index filters: Designing filters with steep skirts, high reflection, and quintic matching layers," *Appl. Opt.*, vol. 35, no. 25, pp. 5191–5196, 1992.

[8] W. H. Southwell, R. L. Hall, and W. J. Gunning, "Using wavelets to design gradient-index interference coatings," in *Proc. SPIE Inhomogeneous and Quasi- Inhomogeneous Optical Coatings*, J. A. Dobrowolski and P. G. Verly, Eds. PQ, Canada, 1993, vol. 2046, pp. 46–49.

[9] S. Martin, A. Brunet-Bruneau, and J. Rivory, "Darwinian evolution of homogeneous multilayer systems," in *Proc. SPIE Optical Interference Coatings*, vol. 2253, F. Abelès, Ed., Grenoble, France, 1994, pp. 168–174.

[10] K. F. Man, K. S. Tang, S. Kwong, and W. A. Halang, *Genetic Algorithms for Control and Signal Processing*, ser. Springer-Verlag Series, K. F. Man, Ed. New York, 1997.

[11] J. A. Dobrowolski, F. C. Ho, A. Belkind, and V. A. Moss, "Merit functions for more effective thin film calculations," *Appl. Opt.*, vol. 28, no. 14, pp. 2824–2831, 1989.

[12] W. H. Southwell and R. H. Hall, "Rugate filter sidelobe suppression using quintic and rugated quintic matching layers," *Appl. Opt.*, vol. 28, no. 14, pp. 2949–2951, 1989.

[13] P. V. Bulkin, P. L. Swart, and B. M. Lacquet, "Electron cyclotron resonance plasma enhanced chemical vapor deposition and optical properties of SiO_x thin films," *J. Non-Cryst. Sol.*, vol. 226, pp. 58–66, 1998.

[14] P. L. Swart, P. V. Bulkin, and B. M. Lacquet, "Rugate filter manufacturing by electron-cyclotron resonance plasma enhanced chemical vapor deposition of SiN_x," *Opt. Eng.*, vol. 36, no. 4, pp. 1214–1219, 1997.

[15] P. Yeh, *Optical Waves in Layered Media*. New York: Wiley, 1988.

[16] A. V. Tikhonravov, "Some theoretical aspects of thin-film optics and their applications," *Appl. Opt.*, vol. 32, no. 28, pp. 5417–5426, 1993.

[17] G. R. Cooper and C. D. McGillem, *Probabilistic Methods of Signal and System Analysis*, 2nd ed. New York: Holt, Rinehart, and Winston, 1986, p. 373.

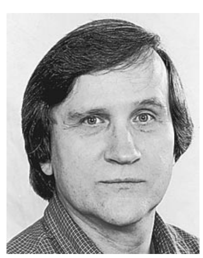

Pieter L. Swart received the B.Sc.Ing. degree (Honors) in electrical engineering (cum laude) and the M.Sc.Ing. degree in electrical engineering (cum laude) from the University of Pretoria, South Africa, in 1967 and 1968, respectively. He received the Ph.D. degree in electrical engineering from McMaster University, Hamilton, ON, Canada, in 1971.

From 1971 to 1972, he was a Natural Sciences and Engineering Research Council Postdoctoral Fellow at The University of British Columbia, Vancouver, Canada. In 1972, he became a Senior Research Associate in the Department of Electrical and Electronic Engineering of the Rand Afrikaans University (RAU), Johannesburg, South Africa, where he is now a Professor and Program Director of the Sensors Sources and Signal Processing Research Group and the Head of the Centre for Optical Communications. He had been Visiting Professor at Carlton University, Ottawa, ON, Canada; McMaster University, Hamilton, ON, Canada; the University of California, Santa Barbara; and the University of British Columbia.

Dr. Swart was awarded several prestigious scholarships. He also received "The Inventor" Insignia by the Canadian Patents and Development Ltd., in 1973, the 1983 Committee Prize Paper Award of the Power Systems Technologies Committee, Industrial Power Systems Department of the IEEE Industry Applications Society, and the Grinaker System Technologies (GST) Award for Excellence (1989). In 1995, he was rated as an A-category Researcher by the Foundation for Research Development in South Africa.

Abraham P. Kotzé received the B.Ing. degree in electrical and electronic engineering from Rand Afrikaans University (RAU), Johannesburg, South Africa, in 1996 and the M.Ing. degree (cum laude) from the same university in 1998 based on a thesis entitled "A comparison of design techniques for gradient-index thin film optical filters." He is presently working toward the D.Ing. degree in optical communications at RAU.

In 1997, he spend three months as a Visiting Research Assistant at the Laboratory for Lightwave Technology at Brown University, Providence, RI.

Mr. Kotzé was the winner of the prestigious National Goldfields Engineering Award for an undergraduate project in 1997.

Beatrys M. Lacquet received the B.Sc. (Hons), M.Ing. (cum laude), and the D.Ing. degrees in electrical and electronic engineering from Rand Afrikaans University (RAU), Johannesburg, South Africa, in 1980, 1984, and 1988, respectively.

In 1990, she worked at the Microsystems Technology Laboratories at the Massachusetts Institute of Technology (MIT), Cambridge, as a Visiting Engineer and was a Visiting Professor at the University of Alberta, Canada, and the Telecommunications Research Laboratories in Edmonton, Alta, Canada, in 1996. She is currently Professor of Electrical and Electronic Engineering at RAU. Her research interests are in the fields of sensors, signal processing, nondestructive measurement techniques, and optical communications.

Dr. Lacquet received the SAMES Best Paper Award for work based on her master's thesis in 1984 and the President's Award of the SAIEE in 1994.